THE JOURNAL OF PHYSICAL CHEMISTRY C

Article

pubs.acs.org/JPCC

Electrically Driven Spin Currents in DNA

Dhurba Rai* and Michael Galperin*

Department of Chemistry & Biochemistry, University of California San Diego, La Jolla, California 92093, United States

ABSTRACT: We consider the generation of pure spin currents by electric field driving. First, we discuss the possibility of spin pumping by electric field within a simple two-level bridge model. Then, we apply the scheme to study spin transport in single- and double-stranded DNA junctions. Within a physically relevant range of parameters we show the possibility of generating pure spin currents in DNA, even in the absence of spin−orbit coupling.

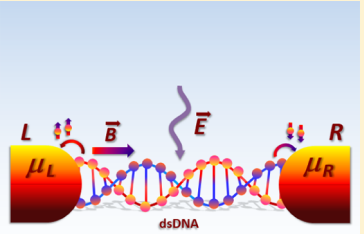

INTRODUCTION

Starting from the pioneering paper on molecular rectifiers,[1] charge transport in junctions is in the center of research in the field of molecular electronics. The development of experimental techniques[2−11] gradually shifted the focus of theoretical research from elastic[12] to inelastic transport,[13−15] to thermoelectric characteristics[16,17] and optical properties[18−20] of molecular junctions. Studies of driving by external fields facilitated the development of methodologies applicable to time-dependent transport.[21−26] In particular, periodically driven junctions received special attention, where numerically exact approaches based on Floquet theory were formulated.[27−34]

Recently, spin transport in molecular devices has started to attract the attention of researchers. The possibility of constructing spin devices utilizing organic molecules was demonstrated in a number of experiments,[35−42] indicating the emergence of molecular spintronics as a new branch of molecular electronics.[43−55] Magnetic field and electric potential[56−60] were considered in the literature as controls for spin flux. Spin−orbit interaction is an ingredient employed in many spin pumps considerations.[58,61−64]

DNA is an important biomolecule, which attracted special attention in the field of molecular electronics. Electron-transfer and -transport properties of DNA spurred intense debate with many experimental[65−70] and theoretical[71−74] studies aimed at elucidating conductance properties of the molecule. Scanning tunneling conductance measurements were proposed[75−77] and realized[78,79] as a tool for determining DNA sequencing.

Recently, spin selectivity in electron transmission through DNA monolayers was measured.[80] Spin polarization was observed for photoelectrons generated with unpolarized light. Later, spin selectivity was also observed for conduction through double-stranded DNA (dsDNA),[81] suggesting the possibility to use DNA as an organic spin filter. A number of theoretical studies attributed the effect to the Rashba spin−orbit coupling (SOC).[82−87] Theoretical analysis, based on second quantization of SOC developed in ref 88, showed that spin selectivity is possible only in double-stranded DNA and only in the presence of dephasing.[84] It was argued that the chiral structure of DNA causes a significant coupling between the particle's momentum and its spin, even if the atom's SOC is small.[89] Also, a possibility to significantly enhance spin polarization by gate voltage was proposed in ref 90.

Here we discuss the possibility to generate pure spin currents through DNA under external electric driving. The proposed scheme allows us to generate spin currents in both single- and double-stranded DNA. After introducing the model in the next section, we present the spin-pumping scheme for a molecular bridge. Then, the scheme is applied to ssDNA and dsDNA junctions. Numerical results obtained for realistic parameters suggest the possibility to generate pure spin currents in the junctions.

MODEL AND METHOD

We use a model for DNA coupled to two metallic leads (L and R) employed previously in refs 84 and 90. The DNA is represented by one (ssDNA) or two (dsDNA) tight-binding chains characterized by their on-site energies $\varepsilon^{(b)}$ and nearest-neighbor electron-hopping $t^{(b)}$ parameters. In the case of the dsDNA, also interchain electron hopping parameter $t^{(12)}$ is employed. The DNA is oriented along the z axis (see Figure 1) and is characterized by the twist angle $\Delta\phi = \pi/5$ between the neighboring base pairs (sites) on the chain and helix angle $\theta \approx 0.66$ rad between the chain and xy plane. SOC on a grid can be derived along the lines presented in ref 91 and is characterized by the parameter t_{SO}. (Note that realistic value of SOC is an issue of ongoing discussion in the literature.[89] Here we employed the value for t_{SO} presented in ref 84. Results for

Received: April 24, 2013
Revised: May 27, 2013
Published: June 10, 2013

   dx.doi.org/10.1021/jp404066y | J. Phys. Chem. C 2013, 117, 13730−13737

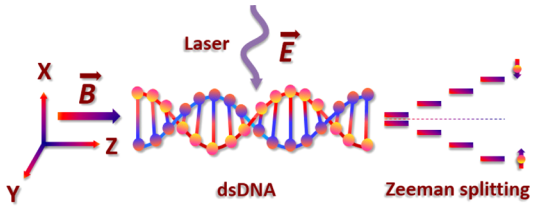

Figure 1. Sketches of the molecular systems (DNA and molecular bridge) driven by dc magnetic, $\vec{B}$, and ac electric, $\vec{E}(t)$, fields.

smaller values of the parameter are also discussed.) This model is complemented by dc magnetic and ac electric fields. Magnetic field induces Zeeman shift to the on-site energies and dresses electron-hopping parameters by a phase. Electric field is coupled via molecular dipole moment. Following ref 28 we consider a local on-site coupling. Contacts L and R are nonmagnetic reservoirs of free charge carriers, each at its own equilibrium.

Hamiltonian of the junction is

$$\hat{H} = \hat{H}_M(t) + \sum_{K=\mathrm{L,R}} (\hat{H}_K + \hat{V}_K) \tag{1}$$

where $\hat{H}_M$, $\hat{H}_K$, and $\hat{V}_K$ are Hamiltonians of the molecule, the contacts, and coupling between them, respectively. Explicit expressions are

$$\begin{aligned}\hat{H}_M(t) = &\sum_{b=1}^{N_b}\sum_{\sigma,\sigma'}\Big(\sum_{m=1}^{N}(\varepsilon^{(b)}_{m,\sigma\sigma'}(t)\hat{d}^{(b)\dagger}_{m\sigma}\hat{d}^{(b)}_{m\sigma'} \\ &+ \delta_{N_b,2}\delta_{\sigma,\sigma'}t^{(b\bar{b})}_m\hat{d}^{(b)\dagger}_{m\sigma}\hat{d}^{(\bar{b})}_{m\sigma}) \\ &+ \sum_{m=1}^{N-1}[(\delta_{\sigma,\sigma'}t^{(b)}_{m,m+1} + it_{SO}[\sigma^{(b)}_{\sigma\sigma'} + \sigma^{(b)}_{m+1,\sigma\sigma'}]) \\ &\times \hat{d}^{(b)\dagger}_{m\sigma}\hat{d}^{(b)}_{m+1\sigma'} + H.\,c.])\end{aligned} \tag{2}$$

$$\hat{H}_K = \sum_{k\in K;\sigma}\varepsilon_k\hat{c}^{\dagger}_{k\sigma}\hat{c}_{k\sigma} \tag{3}$$

$$\hat{V}_K = \sum_{b=1}^{N_b}\sum_{k\in K;\sigma}(V^{(b)}_{mk}\hat{d}^{(b)\dagger}_{m\sigma}\hat{c}_{k\sigma} + H.\,c.) \tag{4}$$

Here b and m number bridges (DNA strands) and site on the bridge, respectively. In the case of two bridges (N_b = 2, i.e., dsDNA), in the molecule $\bar{b}$ is the bridge opposite to b. $d^{(b)\dagger}_{m\sigma}$ and $\hat{c}^{\dagger}_{k\sigma}$ create electron with spin σ on site m of bridge b of the molecule and state k of contacts, respectively. $t^{(b)\bar{b}}_m \equiv t^{(12)}\exp[i\theta_{bm,\bar{b}m}]$ and $t^{(b)}_{m,m+1} \equiv t^{(b)}\exp[i\theta_{bm,bm+1}]$ are electron inter- and intrastrand hopping parameters, respectively, with $\theta_{b_1m_1,b_2m_2} \equiv -|e|(\vec{A}_{b_1m_1} - \vec{A}_{b_2m_2})(\vec{r}_{b_1m_1} + \vec{r}_{b_2m_2})/2\hbar$. (Here $A\rightarrow_{bm}$ is vector potential at the point $\vec{r}_{bm}$.)[92] t_{SO} is the SOC parameter and $\sigma^{(b)}_{m+1,\sigma\sigma'} = \sigma^z_{\sigma\sigma'}\cos\theta - (-1)^b\sin\theta[\sigma^x_{\sigma\sigma'}\sin\phi - \sigma^y_{\sigma\sigma'}\cos\phi]$; here $\vec{\sigma} \equiv \sigma^x$, σ^y, and σ^z are the Pauli matrices, θ is the helix angle, $\phi = m\Delta\phi$, and $\Delta\phi$ is the twist angle.[84] $V^{(b)}_{mk} = \delta_{m,1}V^{(b)}_{Lk}$ for $k \in L$ ($V^{(b)}_{mk} = \delta_{m,N}V^{(b)}_{Rk}$ for $k \in R$) represents electron exchange between contact and molecule. Finally, $\varepsilon^{(b)}_{m,\sigma\sigma'}(t)$ and ε_k are on-site energies for the site m of bridge b in the molecule and state k of contacts, where

$$\varepsilon^{(b)}_{m,\sigma\sigma'}(t) = \delta_{\sigma,\sigma'}[\varepsilon^{(b)} - (\vec{\mu}^{(b)}_m\cdot\vec{E}(t))] - \mu_B(\vec{\sigma}_{\sigma\sigma'}\cdot\vec{B}) \tag{5}$$

Here $\varepsilon^{(b)}$ is on-site energy on bridge b in the absence of fields, $\vec{\mu}^{(b)}_m$ is molecular dipole moment on site m of bridge b, $\vec{E}(t) = (E(t),0,0)$ is the ac electric field, μ_B is the Bohr magneton, and $\vec{B}$ is the dc magnetic field. Equation 5 is the main difference between our model and previous considerations.

Below we consider two different models for the system (see Figure 1): (1) two-level bridge for which we take[93] $\mu^{(b)}_m = \mu_0(N + 1 - 2m)/2$ and (2) DNA where[84] $\mu^{(b)}_m = (-1)^b\,\mu_0\cos[(m-1)\Delta\phi + \phi_0]$. ($\mu_0 \equiv |e|r$ is constant characterizing molecular dipole, e is electron charge, r is either distance between sites, for the bridge model, or radius of the DNA, and ϕ_0 is the angle between the electric field and the first base of the DNA; below we take ϕ_0 = 0.) External electric driving is assumed to be harmonic. Following ref 28 we study monochromatic driving

$$E(t) = E_0\cos(\omega t) \tag{6}$$

and driving by harmonic mixing

$$E(t) = E_0\cos(\omega t) + \frac{E_0}{2}\cos(2\omega t + \varphi) \tag{7}$$

Two types of dc magnetic field are considered: (1) uniform field along the z axis, $\vec{B}$ = (0,0,B) and (2) nonuniform magnetic field, $\vec{B}(\vec{r}) = (-x\kappa/2, -y\kappa/2, z\kappa)$. The latter yields gradient $dB/dz = \kappa$ along the tunneling direction.

Harmonically driven junction, eqs 1−4, is treated within Floquet theory combined with nonequilibrium Green's function formalism.[31] Retarded Green function can be expanded as

$$\mathbf{G}^r(t,t') = \sum_{n=-\infty}^{+\infty}\int_{-\infty}^{+\infty}\frac{dE}{2\pi}\mathbf{G}^r_n(E)e^{-iE(t-t')+in\omega t'} \tag{8}$$

where ω is the fundamental frequency and n is the Floquet index. Coefficients of expansion $\mathbf{G}_n(E) \equiv \mathbf{G}^r_n(E - n\omega) = [\mathrm{G}^a_{-n}(E - n\omega)]^{\dagger}$ satisfy recurrence relations

$$\mathbf{G}_n(E) = \mathbf{G}^{(0)}_n(E)[\delta_{n,0} + \sum_{n'=-\infty}^{+\infty}\mathbf{U}_{n'}\mathbf{G}_{n-n'}(E)] \tag{9}$$

Here $\mathbf{G}^{(0)}_n(E) \equiv \mathbf{G}^{(0)r}(E - n\omega) = [(E - n\omega)\mathbf{I} - \mathbf{H}^{(0)}_M - \Sigma^r(E)]^{-1}$ is the retarded Green function of the system in the absence of driving, $\mathbf{H}^{(0)}_M$ is the molecular Hamiltonian, eq 2, without contribution from electric field $\vec{E}(t)$, and $\Sigma^r(E) \equiv \mathbf{\Sigma}_{K=\mathrm{L,R}}\,\Sigma^r(E)$ is retarded self-energy due to coupling to the contacts. Below we assume a wide-band limit, where

$$[\Sigma^r_K(E)]_{bm\sigma,b'm'\sigma'} = -i\delta_{\sigma,\sigma'}\Gamma^K_{bm,b'm'}/2 \tag{10}$$

does not depend on energy. Here

$$\Gamma^K_{bm,b'm'} \equiv \sum_{k\in K}V^{(b)}_{mk}V^{(b')}_{km'}\delta(E - \varepsilon_k) \tag{11}$$

is the system dephasing matrix due to coupling to contact K. Corresponding advanced self-energy is the Hermitian conjugate of the matrix (10), $\Sigma^a_K(E) = [\Sigma^r_K(E)]^{\dagger}$.

In eq 9, $\mathbf{U}_n$ couples different Floquet indices. In particular, for monochromatic driving, $\mathbf{U}_n = -\delta_{n,\pm1}\mu_M E_0/2$, where $[\mu_M]_{bm\sigma,b'm'\sigma'} = \delta_{b,b'}\delta_{m,m'}\delta_{\sigma,\sigma'}\mu^{(b)}_m$. For harmonic mixing, $\mathbf{U}_n = -\mu_M E_0(\delta_{n,\pm1} + \delta_{n,\pm2}e^{2i\varphi/n}/2)/2$.

The system of eq 9 is matrix relation in molecular orbital, spin, and Floquet spaces, which is solved self-consistently. The (in principle) infinite Floquet space is truncated in practical calculations to account for maximum energy scale relevant for the problem. We find that in our case truncating Floquet space

dx.doi.org/10.1021/jp404066y | J. Phys. Chem. C 2013, 117, 13730−13737

at $n = 20$ yields results that are not sensitive to the space boundary. Once the system of eq 9 is solved, the dc current can be obtained from (see ref 31 for details)

$$I_K^{dc} = -2\mathrm{Re}\int \frac{dE}{2\pi} Tr[G_0(E)\Sigma_K^<(E) + \sum_n \mathbf{G}_n(E)(\Sigma_L^<(E) + \Sigma_R^<(E))G_n^\dagger(E)\Sigma_K^a(E)] \quad (12)$$

Here

$$[\Sigma_K^<(E)]_{bm\sigma,b'm'\sigma'} \equiv i\delta_{\sigma,\sigma'}\Gamma^K_{bm,b'm} f_K(E) \quad (13)$$

is lesser self-energy due to coupling to contact K, and $f_K(E) \equiv [\exp((E - \mu_K)/k_BT) + 1]^{-1}$ is the Fermi-Dirac distribution. Note that under harmonic driving dc components on both interfaces are equal, $I_L^{dc} = I_R^{dc}$. Also note that block-diagonal structure of the self-energies, eqs 10 and 13, in spin space allows us to identify spin-up, $I_\uparrow^{dc}$, and spin-down, $I_\downarrow^{dc}$, components of the total dc current. Thus, we can introduce charge, I_c, and spin, I_s, currents

$$I_c = I_\uparrow^{dc} + I_\downarrow^{dc} \quad (14)$$

$$I_s = I_\uparrow^{dc} - I_\downarrow^{dc} \quad (15)$$

NUMERICAL RESULTS

Here we present numerical results for three models: two-level bridge and single- and double-stranded DNA. The calculations are performed for a physically reasonable set of parameters. Unless stated otherwise, the parameters are $T = 300$ K, $\Gamma_L = \Gamma_R = 0.05$ eV, $\omega = 0.1$ eV, $\varphi = \pi/4$, $\kappa = 8$ mT/nm, and $B = 500$ mT. Fermi energy in the contacts is taken as origin, $E_F = 0$. We note that the parameters are within a physically reasonable range. In particular, escape rates $\Gamma_{L,R}$ are chosen in accordance with experimental data on lifetime for the decay of an excess electron on molecule near-metal surface.[94] Frequency of the electric field is taken in the infrared part of the spectrum, which is in a reasonable range for CO_2 lasers. Finally, magnetic field gradient of several mT/nm were employed in a number of experiments.[95−97] Calculations are performed on energy grid spanning range from −5 to 5 eV with step of 0.05 meV. Floquet space is truncated at $n = 20$.

Two-Level Bridge (TLB). We consider a two-level bridge, $N_b = 1$ and $N = 2$, with on-site energies taken at the origin, $\varepsilon^{(1)} = 0$, and intersite coupling $t^{(1)} = 0.1$ eV. The sites are separated by $r = 7$ nm. Here the goal is to propose a mechanism and check a possibility to generate pure spin currents under electric driving in the absence of spin−orbit interaction.

Charge transfer by external driving was considered for bridge models in ref 28, where necessary conditions to induce charge flux were discussed. In particular, under harmonic driving, eq 6, and for homogeneous $\vec{B}$, the TLB Hamiltonian, eq 2, is symmetric under the generalized parity transformation $\mu_m^{(1)}E(t) \rightarrow \mu_{N-m+1}^{(1)}E(t + \pi/\omega)$. To induce directed charge flux one has to break the symmetry. The latter can be achieved by making level structure of the bridge nonsymmetric (for example, by applying a nonuniform magnetic field) or employing driving by harmonic mixing, eq 7.

To extend the approach to the case of spin pumping, we note that the direction of charge transfer for an asymmetric bridge depends on the position of levels relative to Fermi energy of the contacts. Thus Zeeman splitting around Fermi energy accompanied by magnetic field gradient along the junction is expected to produce spin-polarized currents traveling in the opposite direction in such system, yielding pure spin flux in the junction (i.e., zero total charge flux). Figure 2 demonstrates the

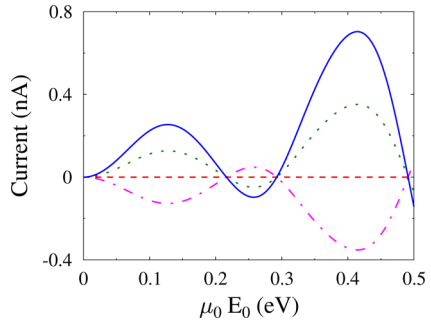

Figure 2. TLB under monochromatic driving, eq 6, in the presence of nonuniform magnetic field. Shown are I_c (dashed line, red), eq 14, I_s (solid line, blue), eq 15, and spin resolved components ($I_\uparrow$, green dotted line and $I_\downarrow$, magenta dashed-dotted line) of the average current, eq 12. See the text for parameters.

effect. One sees that pure spin current is produced as a result of monochromatic electric driving in the presence of nonuniform magnetic field. Charge current across the junction is negligibly small for a wide range of driving amplitudes. Peaks in the dependence on driving amplitude correspond to resonance condition between Rabi frequency of the driving field and positions of eigen-energies of the bridge relative to the Fermi level.[98]

Because symmetric bridges require driving by harmonic mixing to produce directed charge current (see ref 28 for a detailed discussion), we employ eq 7 as a driving force in the presence of uniform magnetic field. Figure 3 demonstrates the possibility of inducing pure spin currents in the presence of uniform magnetic field of 500 mT. In particular, Figure 3a,b shows maps of charge and spin currents, respectively, versus amplitude of driving and position of the level. Regions of small charge current on the map correspond to areas of large spin current. Dashed and dotted lines in Figure 3a indicate paths of $I_c = 0$, and Figure 3c shows a pure spin current along these paths. One sees that also in the presence of uniform magnetic field pure spin current in the nanoampere range can be generated by electric driving within resonable range of parameters. However, pure spin current generation is possible in this case only for low temperatures. (We take $T = 0.5$ K in the calculation.) The reason is absence of time-reversal symmetry under driving by harmonic mixing, which results in the necessity to shift positions of both spin channels to one side relative to the Fermi energy. Thus, to produce charge pumping in opposite directions in the two spin channels, Fermi distributions in the contacts have to be sharp enough to resolve Zeeman splitting in the bridge.

Single-Stranded DNA (ssDNA). Having established the possibility of pure spin-current generation under electric driving in a simple bridge model, we now consider driving spin currents in DNA molecules. We start with the ssDNA, $N_b = 1$ and $N = 10$, and employ electronic structure parameters from ref 84. In particular, we study the strand characterized by $\varepsilon^{(1)} = 0$, $t^{(1)} = 0.12$ eV, and $t_{SO} = 0.01$ eV. The distance between sites of the strand along the helix is 0.56 nm; separation along the z axis is 0.34 nm. (See figure 1 of ref 84 for a sketch.)

dx.doi.org/10.1021/jp404066y | J. Phys. Chem. C 2013, 117, 13730−13737

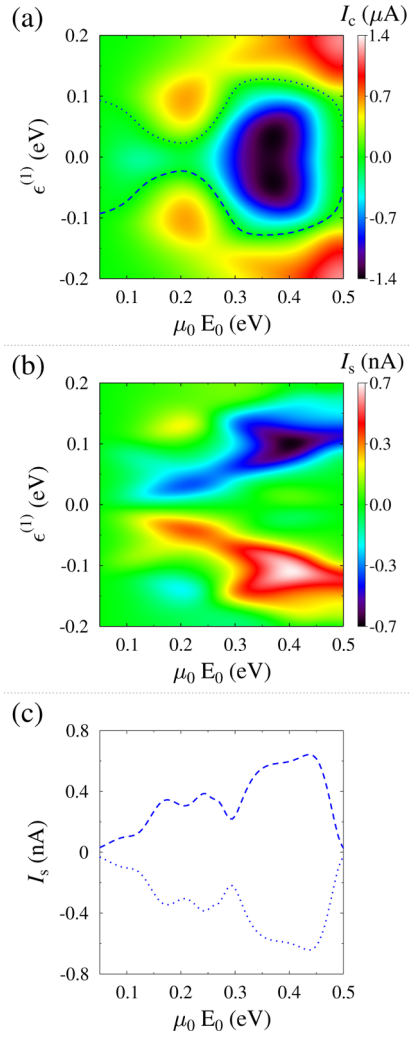

Figure 3. TLB under driving by harmonic mixing, eq 7, in the presence of uniform magnetic field. Shown are maps of (a) I_c, eq 14, and (b) I_s, eq 15, currents versus driving amplitude and position of the levels. Dotted and dashed paths in panel a show $I_c = 0$. Pure spin currents along these paths are presented in panel c. See the text for parameters.

In ssDNA the generalized parity transformation (see the discussion above) takes the form $\mu_m^{(1)}E(t) \rightarrow \mu_{m-[\pi/2\Delta\phi]}^{(1)}E(t + \pi/\omega)$, and thus inducing spin pumping in ssDNA is feasible because even before applying either nonuniform magnetic field or harmonic driving by mixing the parity is broken by the structure of the model. Indeed $[\pi/2\Delta\phi] \equiv [2.5] = 0$; that is, ssDNA helix does not have a site at a position m', making transformation $\mu_m \rightarrow -\mu_{m'}$ possible.

Figure 4 shows currents in ssDNA under monochromatic driving, eq 6. Similar to the two-level model, pure spin current can be generated in the ssDNA junction in the presence of nonuniform magnetic field. (See Figure 4a.) Also, here pure spin current on the order of a fraction of a nanoampere is achievable for a wide range of physically reasonable driving amplitudes. Note that currents of this (or smaller, picoampere) magnitude are experimentally measurable.[67,70] Note also that the calculation is preformed in the absence of SOC, $t_{SO} = 0$. As in the TLB model, peaks in the spin current correspond to resonance conditions between Rabi frequency of the driving and eigenenergies (relative to Fermi) of the DNA.

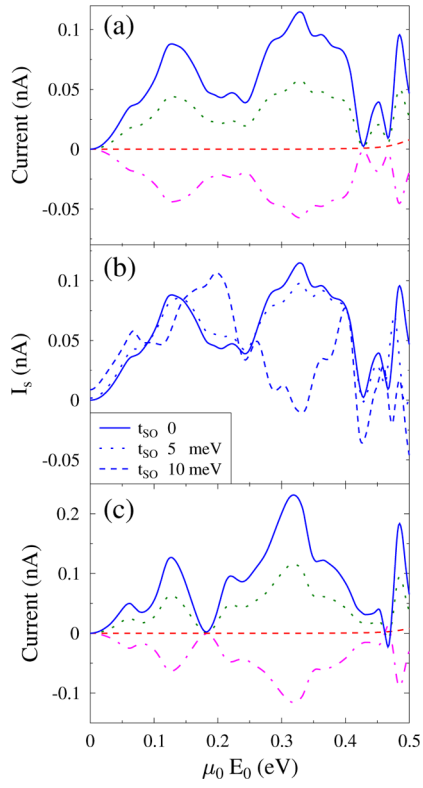

Figure 4. ssDNA under monochromatic driving, eq 6. Shown are I_c (dashed line, red), eq 14, I_s (solid line, blue), eq 15, and spin-resolved components ($I_\uparrow$, green dotted line and $I_\downarrow$, magenta dashed-dotted line) of the average current, eq 12, in the presence of nonuniform (a,b), and uniform (c) magnetic field. In panels a and c, $t_{SO} = 0$; panel b shows I_s for several values of t_{SO}. See the text for other parameters.

The effect of spin−orbit interaction on spin currents through the ssDNA junction is demonstrated in Figure 4b. We see that (at least in the region of low amplitudes) this influence is marginal, which demonstrates that spin pumping is not related to spin−orbit interaction. We attribute the effect to discussion in ref 84, where time-reversal symmetry (in the absence of magnetic field) is discussed for inability of the ssDNA model to behave as a spin filter.

Figure 4c shows currents in ssDNA junction in the presence of uniform magnetic field (B = 500 mT) without SOC (t_{SO} = 0). It is interesting that contrary to the bridge model pure spin current can be induced in ssDNA by monochromatic driving also in the presence of uniform magnetic field. The effect is due to helical structure of DNA molecule, which violates generalized parity condition discussed in ref 28. We note that in the absence of magnetic field no spin pumping is possible (a unitary transformation yields spin-independent form of the ssDNA Hamiltonian, see ref 84 for details); the presence of the field breaks spin symmetry, thus allowing us to use ssDNA as a spin pump.

Driving by harmonic mixing, eq 7, in the presence of uniform magnetic field is shown in Figure 5. Similar to the bridge model, generating pure spin current is possible only at low temperatures, T = 0.5 K, and for a gated electronic structure. Figure 5a demonstrates a map of charge current versus driving amplitude and level position. Paths of $I_c = 0$ are indicated in the map by squares and cicles. Pure spin current along the squares path is shown in Figure 5b to be in the nanoampere range. Note that driving by harmonic mixing does yield spin-polarized

dx.doi.org/10.1021/jp404066y | J. Phys. Chem. C 2013, 117, 13730−13737

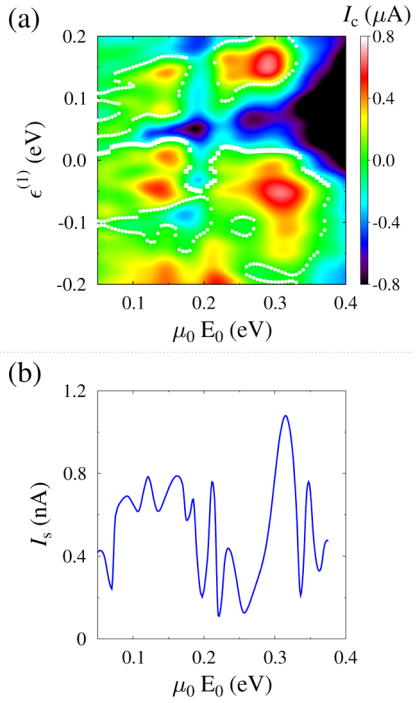

Figure 5. ssDNA under driving by harmonic mixing, eq 7. Shown are (a) map of I_c, eq 14, versus driving amplitude and level position (squares and circles indicate paths of $I_c = 0$) and (b) I_s, eq 15, along the path indicated by squares in panel a. See the text for parameters.

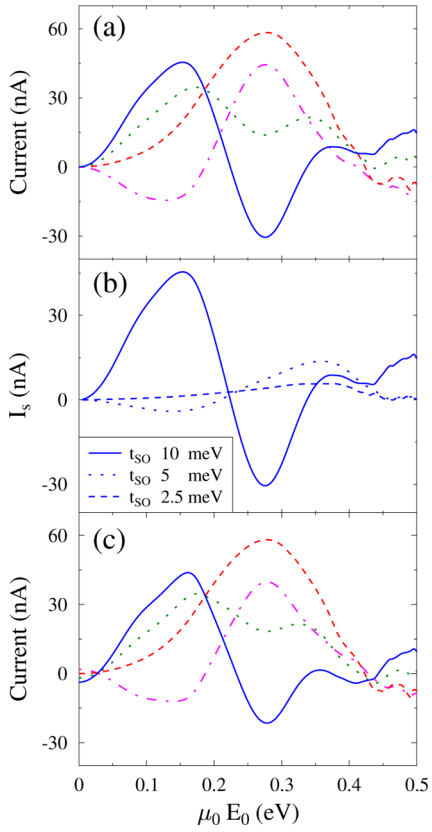

Figure 6. dsDNA under monochromatic driving, eq 6. Shown are I_c (dashed line, red), eq 14, I_s (solid line, blue), eq 15, and spin-resolved components ($I_\uparrow$, green dotted line and $I_\downarrow$, magenta dashed-dotted line) of the average current, eq 12, in the presence of nonuniform (κ = 8 mT/nm) (a,b) and B = 5 T uniform (c) magnetic field. In panels a and c, t_{SO} = 0.01 eV. Panel b shows I_s for several values of t_{SO}. See the text for other parameters.

charge current (not shown) for room temperature and in the absence of gating; however pure spin current cannot be achieved in this regime. Note also that calculations in Figure 5 are performed in the absence of spin−orbit interaction (t_{SO} = 0). Simulations with t_{SO} = 0.01 eV yield similar results. Thus we also see that in the case of driving by harmonic mixing spin pumping is achieved mainly by electric driving.

Double-Stranded DNA (dsDNA). We now study possibility of spin filtering by dsDNA junction, N_b = 2 and N = 10. As previously done, electronic structure parameters are taken from ref 84. In addition to the parameters mentioned in the previous section, we have $\varepsilon^{(2)}$ = 0.3 eV, $t^{(2)}$ = −0.1 eV, and $t^{(12)}$ = −0.3 eV.

Here the generalized parity condition, $\mu_m^{(1)}E(t) \rightarrow \mu_m^{(2)}E(t + \pi/\omega)$, is always fulfilled before nonuniform magnetic field or driving by harmonic mixing is applied. Thus, inducing spin currents in dsDNA by electric driving is expected to be less effective than in ssDNA. Also, because spin filtering by spin−orbit interaction is not excluded in dsDNA by symmetry,[84] we expect it to play an important role here (contrary to the ssDNA case).

Figure 6 presents results for monochromatic driving in dsDNA junction. Similar to ssDNA, spin current can be generated in the presence of both nonuniform (Figure 6a) and uniform (Figure 6c) magnetic fields. However, more complicated electronic structure of dsDNA restricts the generation of pure spin currents ($I_s \gg I_c$) to driving amplitudes below 0.1 eV. Contrary to ssDNA, spin pumping by electric driving in dsDNA junction is defined mainly by SOC for the chosen set of parameters. We attribute this result to the fact that dsDNA (contrary to ssDNA) can behave as a spin filter also in the absence of magnetic field.[84]

Figure 6b shows spin current, I_s, for several choices of this parameter. As strength of the SOC diminishes, so does the value of I_s. For t_{SO} = 0 spin current becomes on the order of nanoamperes, which is similar to the values obtained for ssDNA. (See Figure 4.) Contrary to the latter case the total charge flux in the junction is nonzero. The reason is a more complicated electronic structure of dsDNA, which results in more complex behavior of the resonance conditions[28] with pumping parameters. Pure spin current can still be generated, but one has to add gating to the system. (See Figure 5.)

Finally, Figure 7 shows results for dsDNA junction driven by harmonic mixing. The calculation is performed in the absence of magnetic field. As previously, to get spin currents essentially larger than charge flux, we need to gate the junction and restrict consideration to low temperatures, T = 0.5 K. Figure 7a presents a map of charge current versus driving amplitude and gated position of $\varepsilon^{(1)}$. Paths of I_c = 0 are indicated on the map by squares and circles, and Figure 7b shows pure spin current along the squares path. Note that similar to ssDNA also in this case spin-polarized charge currents can be achieved at room temperature and in the absence of gating.

■ CONCLUSIONS

We considered pure spin current generation by electric field. Monochromatic field and driving by harmonic mixing were discussed. We first studied the possibility of pure spin flux pumping in a simple bridge model. In particular, complementing consideration of ref 28 we showed that the presence of

dx.doi.org/10.1021/jp404066y | J. Phys. Chem. C 2013, 117, 13730−13737

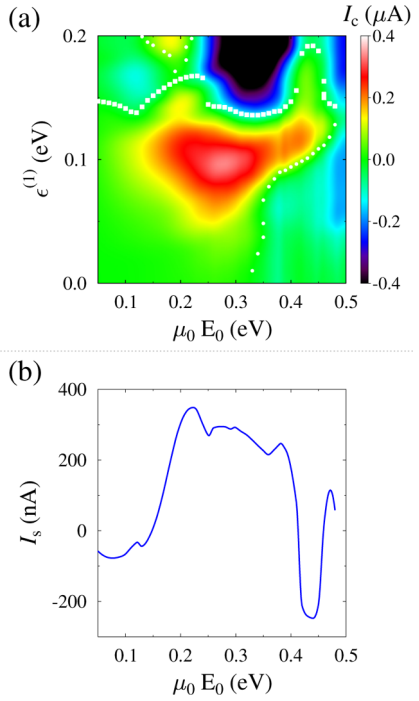

Figure 7. dsDNA under driving by harmonic mixing, eq 7. Shown are (a) map of I_c, eq 14, versus driving amplitude and level position (squares and circles indicate paths of $I_c = 0$) and (b) I_s, eq 15, along the path indicated by squares in panel a. See the text for parameters.

nonuniform (with driving by monochromatic electric field) or uniform (with electric driving by harmonic mixing) magnetic field leads to generation of pure spin currents in linear molecular bridge. We then applied the scheme to the models of single- and double-stranded DNA junctions within realistic range of parameters. Our main conclusions are:

(1) Monochromatic driving is capable of producing pure spin currents on the order of 0.1 nA in ssDNA and 10 nA in dsDNA junctions. We note that currents of 0.1 nA (and lower) orders are experimentally measurable.[67,70]

(2) Driving by harmonic mixing yields pure spin currents ($I_s \gg I_c$) only at very low temperatures and under gating conditions in both ssDNA and dsDNA junctions. However, spin-polarized currents ($I_s \approx I_c$) can be obtained at room temperature and in the absence of gating.

(3) Helical structure of DNA allows the generation of pure spin currents by harmonic driving in the presence of uniform magnetic field. This is in contrast with bridge models, wherein symmetry considerations prohibit pumping.[28]

(4) In ssDNA, spin−orbit interaction plays only a marginal role in spin pumping in the junction. On the contrary in dsDNA SOC plays the main role. We attributed the effect to discussion in ref 84 about the inability of ssDNA to perform as a spin filter: in the absence of magnetic field, time-reversal symmetry makes it impossible to observe spin polarization.

Note that the present consideration is a step aside from the general trend in recent studies of DNA junctions.[82−86,90] Instead of focusing on the spin−orbit interaction (undoubtedly an important ingredient), we propose an alternative setup involving ac electric and dc magnetic fields that allows us to induce measurable spin currents in the system. Parameters for the field strengths are chosen to represent realistic experimental setup, thus demonstrating (albeit in a simple model) feasibility of utilizing DNA structures as spin-filter devices when subjected to external fields. We note that debatable value of the SOC is of secondary importance in our study (at least for the case of ssDNA, where it is shown to play no essential role). The possibility to induce pure and spin-polarized currents even in the absence of the SOC is the main conclusion of our study.

AUTHOR INFORMATION

Corresponding Author

*E-mail: dhrai@ucsd.edu (D.R.); migalperin@ucsd.edu (M.G.). Phone +1 858 246 0511. Fax +1 858 534 6255.

Notes

The authors declare no competing financial interest.

ACKNOWLEDGMENTS

We thank Prof. Abraham Nitzan for helpful discussions. We gratefully acknowledge support by the National Science Foundation (CHE-1057930) and the US-Israel Binational Science Foundation (grant no. 2008282).

REFERENCES

(1) Aviram, A.; Ratner, M. A. Molecular Rectifiers. *Chem. Phys. Lett.* **1974**, *29*, 277−283.

(2) Reed, M. A.; Zhou, C.; Muller, C. J.; Burgin, T. P.; Tour, J. M. Conductance of a Molecular Junction. *Science* **1997**, *278*, 252−254.

(3) Smit, R. H. M.; Noat, Y.; Untiedt, C.; Lang, N. D.; van Hemert, M. C.; van Ruitenbeek, J. M. Measurement of the Conductance of a Hydrogen Molecule. *Nature* **2002**, *419*, 906−909.

(4) Zhitenev, N. B.; Meng, H.; Bao, Z. Conductance of Small Molecular Junctions. *Phys. Rev. Lett.* **2002**, *88*, 226801.

(5) Poot, M.; Osorio, E.; O'Neill, K.; Thijssen, J. M.; Vanmaekelbergh, D.; Walree, C. A. v.; Jenneskens, L. W.; Zant, H. S. J. v. d. Temperature Dependence of Three-Terminal Molecular Junctions with Sulfur End-Functionalized Tercyclohexylidenes. *Nano Lett.* **2006**, *6*, 1031−1035.

(6) Reddy, P.; Jang, S.-Y.; Segalman, R. A.; Majumdar, A. Thermoelectricity in Molecular Junctions. *Science* **2007**, *315*, 1568−1571.

(7) Huang, Z.; Chen, F.; D'agosta, R.; Bennett, P. A.; Di Ventra, M.; Tao, N. Local Ionic and Electron Heating in Single-Molecule Junctions. *Nat. Nanotechnol.* **2007**, *2*, 698−703.

(8) Wang, Z.; Carter, J. A.; Lagutchev, A.; Koh, Y. K.; Seong, N.-H.; Cahill, D. G.; Dlott, D. D. Ultrafast Flash Thermal Conductance of Molecular Chains. *Science* **2007**, *317*, 787−790.

(9) Ioffe, Z.; Shamai, T.; Ophir, A.; Noy, G.; Yutsis, I.; Kfir, K.; Cheshnovsky, O.; Selzer, Y. Detection of Heating in Current-Carrying Molecular Junctions by Raman Scattering. *Nat. Nanotechnol.* **2008**, *3*, 727−732.

(10) Ward, D. R.; Halas, N. J.; Ciszek, J. W.; Tour, J. M.; Wu, Y.; Nordlander, P.; Natelson, D. Simultaneous Measurements of Electronic Conduction and Raman Response in Molecular Junctions. *Nano Lett.* **2008**, *8*, 919−924.

(11) Ward, D. R.; Corley, D. A.; Tour, J. M.; Natelson, D. Vibrational and Electronic Heating in Nanoscale Junctions. *Nat. Nanotechnol.* **2011**, *6*, 33−38.

(12) Nitzan, A.; Ratner, M. A. Electron Transport in Molecular Wire Junctions. *Science* **2003**, *300*, 1384−1389.

(13) Lindsay, S. M.; Ratner, M. A. Molecular Transport Junctions: Clearing Mists. *Adv. Mater.* **2007**, *19*, 23−31.

(14) Galperin, M.; Ratner, M. A.; Nitzan, A.; Troisi, A. Nuclear Coupling and Polarization in Molecular Transport Junctions: Beyond Tunneling to Function. *Science* **2008**, *319*, 1056−1060.

(15) Galperin, M.; Ratner, M. A.; Nitzan, A. Molecular Transport Junctions: Vibrational Effects. *J. Phys.: Condens. Matter* **2007**, *19*, 103201.
(16) Nitzan, A. Molecules Take the Heat. *Science* **2007**, *317*, 759–760.
(17) Fransson, J.; Galperin, M. Spin Seebeck Coefficient of a Molecular Spin Pump. *Phys. Chem. Chem. Phys.* **2011**, *13*, 14350–14357.
(18) Song, P.; Nordlander, P.; Gao, S. Quantum Mechanical Study of the Coupling of Plasmon Excitations to Atomic-Scale Electron Transport. *J. Chem. Phys.* **2011**, *134*, 074701.
(19) Galperin, M.; Nitzan, A. Molecular Optoelectronics: The Interaction of Molecular Conduction Junctions with Light. *Phys. Chem. Chem. Phys.* **2012**, *14*, 9421–9438.
(20) Park, T.-H.; Galperin, M. A Time-Dependent Response to Optical Excitation in Molecular Junctions. *Phys. Scr.* **2012**, *T151*, 014038.
(21) Jauho, A.-P.; Wingreen, N. S.; Meir, Y. Time-Dependent Transport in Interacting and Noninteracting Resonant-Tunneling Systems. *Phys. Rev. B* **1994**, *50*, 5528–5544.
(22) Maciejko, J.; Wang, J.; Guo, H. Time-Dependent Quantum Transport Far from Equilibrium: An Exact Nonlinear Response Theory. *Phys. Rev. B* **2006**, *74*, 085324.
(23) Myöhänen, P.; Stan, A.; Stefanucci, G.; van Leeuwen, R. Kadanoff-Baym Approach to Quantum Transport through Interacting Nanoscale Systems: From the Transient to the Steady-State Regime. *Phys. Rev. B* **2009**, *80*, 115107.
(24) Stan, A.; Dahlen, N. E.; van Leeuwen, R. Time Propagation of the Kadanoff–Baym Equations for Inhomogeneous Systems. *J. Chem. Phys.* **2009**, *130*, 224101.
(25) Sukharev, M.; Galperin, M. Transport and Optical Response of Molecular Junctions Driven by Surface Plasmon Polaritons. *Phys. Rev. B* **2010**, *81*, 165307.
(26) White, A. J.; Sukharev, M.; Galperin, M. Molecular Nanoplasmonics: Self-Consistent Electrodynamics in Current-Carrying Junctions. *Phys. Rev. B* **2012**, *86*, 205324.
(27) Grifoni, M.; Hänggi, P. Driven Quantum Tunneling. *Phys. Rep.* **1998**, *304*, 229–354.
(28) Lehmann, J.; Kohler, S.; Hänggi, P.; Nitzan, A. Rectification of Laser-Induced Electronic Transport through Molecules. *J. Chem. Phys.* **2003**, *118*, 3283–3293.
(29) Kohler, S.; Camalet, S.; Strass, M.; Lehmann, J.; Ingold, G.-L.; Hänggi, P. Charge Transport through a Molecule Driven by a High-Frequency Field. *Chem. Phys.* **2004**, *296*, 243–249.
(30) Kohler, S.; Lehmann, J.; Hänggi, P. Driven Quantum Transport on the Nanoscale. *Phys. Rep.* **2005**, *406*, 379–443.
(31) Stefanucci, G.; Kurth, S.; Rubio, A.; Gross, E. K. U. Time-Dependent Approach to Electron Pumping in Open Quantum Systems. *Phys. Rev. B* **2008**, *77*, 075339.
(32) Wu, B. H.; Cao, J. C. A Floquet-Green's Function Approach to Mesoscopic Transport Under AC Bias. *J. Phys.: Condens. Matter* **2008**, *20*, 085224.
(33) Einax, M.; Solomon, G. C.; Dieterich, W.; Nitzan, A. Unidirectional Hopping Transport of Interacting Particles on a Finite Chain. *J. Chem. Phys.* **2010**, *133*, 054102.
(34) Rohling, N.; Grossmann, F. Optimization of Electron Pumping by Harmonic Mixing. *Phys. Rev. B* **2011**, *83*, 205310.
(35) Bogani, L.; Wernsdorfer, W. Molecular Spintronics Using Single-Molecule Magnets. *Nat. Mater.* **2008**, *7*, 179–186.
(36) Mannini, M.; Pineider, F.; Sainctavit, P.; Danieli, C.; Otero, E.; Sciancalepore, C.; Talarico, A. M.; Arrio, M.-A.; Cornia, A.; Gatteschi, D.; Sessoli, R. Magnetic Memory of a Single-Molecule Quantum Magnet Wired to a Gold Surface. *Nat. Mater.* **2009**, *8*, 194–197.
(37) Wernsdorfer, W. Molecular Nanomagnets: Towards Molecular Spintronics. *Int. J. Nanotechnol.* **2010**, *7*, 497–522.
(38) Urdampilleta, M.; Nguyen, N.-V.; Cleuziou, J.-P.; Klyatskaya, S.; Ruben, M.; Wernsdorfer, W. Molecular Quantum Spintronics: Supramolecular Spin Valves Based on Single-Molecule Magnets and Carbon Nanotubes. *Int. J. Mol. Sci.* **2011**, *12*, 6656–6667.
(39) Urdampilleta, M.; Klyatskaya, S.; Cleuziou, J.-P.; Ruben, M.; Wernsdorfer, W. Supramolecular Spin Valves. *Nat. Mater.* **2011**, *10*, 502–506.
(40) Schwobel, J.; Fu, Y.; Brede, J.; Dilullo, A.; Hoffmann, G.; Klyatskaya, S.; Ruben, M.; Wiesendanger, R. Real-Space Observation of Spin-Split Molecular Orbitals of Adsorbed Single-Molecule Magnets. *Nat. Commun.* **2012**, *3*, 953.
(41) Ganzhorn, M.; Klyatskaya, S.; Ruben, M.; Wernsdorfer, W. Strong Spin-Phonon Coupling Between a Single-Molecule Magnet and a Carbon Nanotube Nanoelectromechanical System. *Nat. Nanotechnol.* **2013**, *8*, 165–169.
(42) Raman, K. V.; Kamerbeek, A. M.; Mukherjee, A.; Atodiresei, N.; Sen, T. K.; Lazic, P.; Caciuc, V.; Michel, R.; Stalke, D.; Mandal, S. K.; Blugel, S.; Munzenberg, M.; Moodera, J. S. Interface-Engineered Templates for Molecular Spin Memory Devices. *Nature* **2013**, *493*, 509–513.
(43) Rocha, A. R.; Garcia-suarez, V. M.; Bailey, S. W.; Lambert, C. J.; Ferrer, J.; Sanvito, S. Towards Molecular Spintronics. *Nat. Mater.* **2005**, *4*, 335–339.
(44) Sanvito, S.; Rocha, A. Molecular-Spintronics: The Art of Driving Spin through Molecules. *J. Comput. Theor. Nanosci.* **2006**, *3*, 624–642.
(45) Tyagi, P. Molecular Spin Devices: Current Understanding and New Territories. *Nano* **2009**, *4*, 325–338.
(46) Kim, W. Y.; Kim, K. S. Tuning Molecular Orbitals in Molecular Electronics and Spintronics. *Acc. Chem. Res.* **2010**, *43*, 111–120.
(47) Zhu, L.; Yao, K. L.; Liu, Z. L. Molecular Spin Valve and Spin Filter Composed of Single-Molecule Magnets. *Appl. Phys. Lett.* **2010**, *96*, 082115.
(48) Soncini, A.; Chibotaru, L. F. Molecular Spintronics Using Noncollinear Magnetic Molecules. *Phys. Rev. B* **2010**, *81*, 132403.
(49) Herrmann, C.; Solomon, G. C.; Ratner, M. A. Organic Radicals As Spin Filters. *J. Am. Chem. Soc.* **2010**, *132*, 3682–3684.
(50) Soncini, A.; Mallah, T.; Chibotaru, L. F. Molecular Spintronics in Mixed-Valence Magnetic Dimers: The Double-Exchange Blockade Mechanism. *J. Am. Chem. Soc.* **2010**, *132*, 8106–8114.
(51) Sanvito, S. Molecular Spintronics: The Rise of Spinterface Science. *Nat. Phys.* **2010**, *6*, 562–564.
(52) Sanvito, S. Organic Spintronics: Filtering Spins with Molecules. *Nat. Mater.* **2011**, *10*, 484–485.
(53) Herrmann, C.; Solomon, G. C.; Ratner, M. A. Designing Organic Spin Filters in the Coherent Tunneling Regime. *J. Chem. Phys.* **2011**, *134*, 224306.
(54) Sanvito, S. Molecular Spintronics. *Chem. Soc. Rev.* **2011**, *40*, 3336–3355.
(55) Winpenny, R. E. P. Molecular Spintronics: Stretch for a Moment. *Nat. Nanotechnol.* **2013**, *8*, 159–160.
(56) Wang, B.; Wang, J.; Guo, H. Quantum Spin Field Effect Transistor. *Phys. Rev. B* **2003**, *67*, 092408.
(57) Sun, Q.-f.; Guo, H.; Wang, J. A Spin Cell for Spin Current. *Phys. Rev. Lett.* **2003**, *90*, 258301.
(58) Wu, B. H.; Ahn, K.-H. Proposal For an Electrical Spin Cell With Single Barrier. *Appl. Phys. Lett.* **2006**, *88*, 142101.
(59) Braun, M.; Burkard, G. Nonadiabatic Two-Parameter Charge and Spin Pumping in a Quantum Dot. *Phys. Rev. Lett.* **2008**, *101*, 036802.
(60) Fransson, J.; Galperin, M. Inelastic Scattering and Heating in a Molecular Spin Pump. *Phys. Rev. B* **2010**, *81*, 075311.
(61) Governale, M.; Taddei, F.; Fazio, R. Pumping Spin With Electrical Fields. *Phys. Rev. B* **2003**, *68*, 155324.
(62) Wu, B. H.; Cao, J. C. Time-Dependent Multimode Transport through Quantum Wires With Spin-Orbit Interaction: Floquet Scattering Matrix Approach. *Phys. Rev. B* **2006**, *73*, 245412.
(63) Pan, H.; Zhao, Y. Spin Pumping and Spin Filtering in Double Quantum Dots with Time-Dependent Spin-Orbit Interactions. *J. Appl. Phys.* **2012**, *111*, 083703.
(64) Wang, Y.-X.; Wu, Y.-M.; Xiong, S.-J. Spin Current Pumping with Two Orthogonal Electric Fields in Quantum Wire. *Phys. B* **2012**, *407*, 4425–4429.

(65) Okahata, Y.; Kobayashi, T.; Tanaka, K.; Shimomura, M. Anisotropic Electric Conductivity in an Aligned DNA Cast Film. *J. Am. Chem. Soc.* **1998**, *120*, 6165−6166.
(66) Fink, H.-W.; Schonenberger, C. Electrical Conduction through DNA Molecules. *Nature* **1999**, *398*, 407−410.
(67) Porath, D.; Bezryadin, A.; de Vries, S.; Dekker, C. Direct Measurement of Electrical Transport through DNA Molecules. *Nature* **2000**, *403*, 635−638.
(68) Xu, B.; Zhang, P.; Li, X.; Tao, N. Direct Conductance Measurement of Single DNA Molecules in Aqueous Solution. *Nano Lett.* **2004**, *4*, 1105−1108.
(69) Cohen, H.; Nogues, C.; Naaman, R.; Porath, D. Direct Measurement of Electrical Transport through Single DNA Molecules of Complex Sequence. *Proc. Natl. Acad. Sci.* **2005**, *102*, 11589−11593.
(70) Roy, S.; Vedala, H.; Roy, A. D.; Kim, D.-h.; Doud, M.; Mathee, K.; Shin, H.-k.; Shimamoto, N.; Prasad, V.; Choi, W. Direct Electrical Measurements on Single-Molecule Genomic DNA Using Single-Walled Carbon Nanotubes. *Nano Lett.* **2008**, *8*, 26−30.
(71) Jortner, J.; Bixon, M.; Langenbacher, T.; Michel-Beyerle, M. E. Charge Transfer and Transport in DNA. *Proc. Natl. Acad. Soc.* **1998**, *95*, 12759−12765.
(72) Bixon, M.; Giese, B.; Wessely, S.; Langenbacher, T.; Michel-Beyerle, M. E.; Jortner, J. Long-Range Charge Hopping in DNA. *Proc. Natl. Acad. Soc.* **1999**, *96*, 11713−11716.
(73) Bixon, M.; Jortner, J. Long-Range and Very Long-Range Charge Transport in DNA. *Chem. Phys.* **2002**, *281*, 393−408.
(74) Malyshev, A. V. DNA Double Helices for Single Molecule Electronics. *Phys. Rev. Lett.* **2007**, *98*, 096801.
(75) Zwolak, M.; Di Ventra, M. Electronic Signature of DNA Nucleotides via Transverse Transport. *Nano Lett.* **2005**, *5*, 421−424.
(76) Lagerqvist, J.; Zwolak, M.; Di Ventra, M.; Fast, D. N. A. Sequencing via Transverse Electronic Transport. *Nano Lett.* **2006**, *6*, 779−782.
(77) Zwolak, M.; Di Ventra, M. *Colloquium*: Physical Approaches to DNA Sequencing and Detection. *Rev. Mod. Phys.* **2008**, *80*, 141−165.
(78) Huang, S.; He, J.; Chang, S.; Zhang, P.; Liang, F.; Li, S.; Tuchband, M.; Fuhrmann, A.; Ros, R.; Lindsay, S. Identifying Single Bases in a DNA Oligomer with Electron Tunnelling. *Nat. Nanotechnol.* **2010**, *5*, 868−873.
(79) Ivanov, A. P.; Instuli, E.; McGilvery, C. M.; Baldwin, G.; McComb, D. W.; Albrecht, T.; Edel, J. B. DNA Tunneling Detector Embedded in a Nanopore. *Nano Lett.* **2011**, *11*, 279−285.
(80) Göhler, B.; Hamelbeck, V.; Markus, T. Z.; Kettner, M.; Hanne, G. F.; Vager, Z.; Naaman, R.; Zacharias, H. Spin Selectivity in Electron Transmission through Self-Assembled Monolayers of Double-Stranded DNA. *Science* **2011**, *331*, 894−897.
(81) Xie, Z.; Markus, T. Z.; Cohen, S. R.; Vager, Z.; Gutierrez, R.; Naaman, R. Spin Specific Electron Conduction through DNA Oligomers. *Nano Lett.* **2011**, *11*, 4652−4655.
(82) Yeganeh, S.; Ratner, M. A.; Medina, E.; Mujica, V. Chiral Electron Transport: Scattering through Helical Potentials. *J. Chem. Phys.* **2009**, *131*, 014707.
(83) Gutierrez, R.; Díaz, E.; Naaman, R.; Cuniberti, G. Spin-Selective Transport through Helical Molecular Systems. *Phys. Rev. B* **2012**, *85*, 081404.
(84) Guo, A.-M.; Sun, Q.-f. Spin-Selective Transport of Electrons in DNA Double Helix. *Phys. Rev. Lett.* **2012**, *108*, 218102.
(85) Guo, A.-M.; Sun, Q.-f. Sequence-Dependent Spin-Selective Tunneling along Double-Stranded DNA. *Phys. Rev. B* **2012**, *86*, 115441.
(86) Medina, E.; López, F.; Ratner, M. A.; Mujica, V. Chiral Molecular Films as Electron Polarizers and Polarization Modulators. *Europhys. Lett.* **2012**, *99*, 17006.
(87) Diniz, G. S.; Latgé, A.; Ulloa, S. E. Helicoidal Fields and Spin Polarized Currents in Carbon Nanotube-DNA Hybrids. *Phys. Rev. Lett.* **2012**, *108*, 126601.
(88) Sun, Q.-f.; Wang, J.; Guo, H. Quantum Transport Theory for Nanostructures with Rashba Spin-Orbital Interaction. *Phys. Rev. B* **2005**, *71*, 165310.
(89) Naaman, R.; Waldeck, D. H. Chiral-Induced Spin Selectivity Effect. *J. Phys. Chem. Lett.* **2012**, *3*, 2178−2187.
(90) Guo, A.-M.; Sun, Q.-f. Enhanced Spin-Polarized Transport through DNA Double Helix by Gate Voltage. *Phys. Rev. B* **2012**, *86*, 035424.
(91) Sun, Q.-f.; Xie, X. C.; Wang, J. Persistent Spin Current in Nanodevices and Definition of the Spin Current. *Phys. Rev. B* **2008**, *77*, 035327.
(92) Rai, D.; Hod, O.; Nitzan, A. Magnetic Fields Effects on the Electronic Conduction Properties of Molecular Ring Structures. *Phys. Rev. B* **2012**, *85*, 155440.
(93) Lehmann, J.; Kohler, S.; Hänggi, P.; Nitzan, A. Molecular Wires Acting as Coherent Quantum Ratchets. *Phys. Rev. Lett.* **2002**, *88*, 228305.
(94) Kinoshita, I.; Misu, A.; Munakata, T. Electronic Excited State of NO Adsorbed on Cu(111): A Two-Photon Photoemission Study. *J. Chem. Phys.* **1995**, *102*, 2970.
(95) Degen, C. L.; Poggio, M.; Mamin, H. J.; Rettner, C. T.; Rugar, D. Nanoscale Magnetic Resonance Imaging. *Proc. Natl. Acad. Sci.* **2009**, *106*, 1313−1317.
(96) Longenecker, J. G.; Mamin, H. J.; Senko, A. W.; Chen, L.; Rettner, C. T.; Rugar, D.; Marohn, J. A. High-Gradient Nanomagnets on Cantilevers for Sensitive Detection of Nuclear Magnetic Resonance. *ACS Nano* **2012**, *6*, 9637−9645.
(97) Mamin, H. J.; Rettner, C. T.; Sherwood, M. H.; Gao, L.; Rugar, D. High Field-Gradient Dysprosium Tips for Magnetic Resonance Force Microscopy. *Appl. Phys. Lett.* **2012**, *100*, 013102.
(98) Peskin, U.; Galperin, M. Coherently Controlled Molecular Junctions. *J. Chem. Phys.* **2012**, *136*, 044107.